

# RF Characteristics of Poly-Si TFTs with HfO<sub>2</sub> Gate Dielectric Fabricated by Microwave Annealing

Jia-Jin Tsai and Hsin-Hui Hu

Department of Electronic Engineering, National Taipei University of Technology, Taipei 106, Taiwan, R.O.C.  
Phone: +886-2-27712171 ext. 2287 E-mail: hhu@ntut.edu.tw

## Abstract

This work presents the RF characteristics of the poly-Si TFTs with high- $\kappa$  HfO<sub>2</sub> gate dielectric annealed by low-temperature MWA. The cutoff frequency ( $f_T$ ) and oscillation frequency ( $f_{max}$ ) of poly-Si TFTs with different layout structures, including annular, single, and parallel are investigated. The annular layout structure with  $L=150$  nm has a higher  $f_T$  (1.69 GHz). Results show that the poly-Si TFT technique can feasibly be utilized in system-on-panel applications.

## 1. Introduction

Polycrystalline silicon thin-film transistors (poly-Si TFTs) have higher electron mobility and driving current than amorphous silicon TFTs and have potential for RF applications [1-3]. The RF performance is expected to improve with scaling. However, continuous shrinking of device is facing several challenges, such as short channel effects (SCEs) and high gate leakage current. It has been reported that low-temperature microwave annealing (MWA) technique can restrain the dopant diffusion and suppress the short channel effects [4-5]. In addition, poly-Si TFTs with high- $\kappa$  gate dielectric have been proposed to have lower gate-leakage current and better electrical characteristics than with SiO<sub>2</sub> gate dielectric [6-7]. Therefore, in this work, poly-Si TFTs with high- $\kappa$  HfO<sub>2</sub> gate dielectric annealed by MWA are fabricated. The high-frequency characteristics of poly-Si TFTs with different layout structures are studied.

## 2. Experiments

Fig. 1 shows the top-view SEM images of poly-Si TFTs with different layout structures, including annular, single, and parallel. The gate length ( $L$ ) of poly-Si TFTs are 105 nm as shown in Fig. 1(d). The total gate-width of devices in this work are fixed at 44  $\mu$ m for comparison. A 100-nm thick layer of active is a solid-phase-crystallized poly-Si film. A 50-nm thick TiN layer and a 4-nm-thick HfO<sub>2</sub> layer act as the metal gate electrode and gate dielectric, respectively. Low-temperature MWA for dopant activation is performed at 3 kW for 300 sec.

## 3. Results and Discussion

Fig. 2 shows  $I_{DS}-V_{GS}$  transfer curves of poly-Si TFTs with different layout structures. The DC characteristics of these three structures are similar. In Fig. 3, the cutoff frequency ( $f_T$ ) of the annular one is obviously higher than the others. Since the usual approximation for  $f_T$  is  $g_m/2\pi(C_{gs}+C_{gd})$ , the small-

signal parameters are extracted and analyzed. Fig. 4 and Fig. 5 show the extracted transconductance ( $g_m$ ) and gate parasitic capacitances ( $C_{gs}$ ,  $C_{gd}$ ) for all devices. Although the  $g_m$  value of the annular one is not the highest, the  $C_{gs}$  and  $C_{gd}$  of the annular one are the smallest. Therefore, the annular one has the highest  $f_T$ . In Fig. 5, the parallel one has higher  $C_{gs}$  and  $C_{gd}$  than the single one due to stripe-shape gate configuration. Hence, the better  $f_T$  of the parallel one than of the single one is attributed to the higher  $g_m$  in the parallel one than in the single one. Fig. 6 shows the oscillation frequency ( $f_{max}$ ) of all devices. The approximation for  $f_{max}$  can be expressed as follows [8]:

$$f_{max} \sim \frac{f_T}{\sqrt{4g_{DS}R_g + 8\pi f_T C_{gd}(R_g + \alpha R_d)}}$$

The  $f_{max}$  is proportional to the  $f_T$  and is strongly related to the gate resistance ( $R_g$ ). The extracted  $R_g$  for all devices is show in Fig.7. Although the  $R_g$  value of the annular one is not the lowest, the  $f_T$  of the annular one is the highest. Therefore, the annular one has the highest  $f_{max}$ . As for the single and parallel layout structures, with a constant total gate-width, the  $R_g$  values decrease as the finger width increase. Hence, the parallel one has higher  $f_{max}$  than the single one. Fig. 8 shows the peak  $f_T$  values of all devices before and after sintering. The enhanced  $f_T$  after sintering is attributed to the passivation of grain boundary defects and poly-Si/interfacial oxide interface states [7]. After sintering, the peak  $f_T$  of the annular one with  $L = 150$  nm is 1.69 GHz.

## 4. Conclusions

The high-frequency performance of poly-Si TFTs with HfO<sub>2</sub> gate dielectric annealed by MWA are investigated. The annular layout structure exhibits higher  $f_T$  and  $f_{max}$  than the other layout types. Additionally, poly-Si TFT with  $L = 105$  nm still has acceptable switching characteristics due to low-temperature MWA which restrain the dopant diffusion. Consequently, the RF performance can be improved by shrinking the gate length in conjunction with MWA.

## References

- [1] J. L. Botrel *et al.*, *Thin Solid Films* **515** (2007) 7422.
- [2] Y. J. E. Chen *et al.*, *IEEE Trans. Microw. Theory Tech.* **58** (2010) 3444.
- [3] S. Y. Kim *et al.*, *IEEE Trans. Electron Devices* **59** (2012) 2296.
- [4] T. L. Alford *et al.*, *J. Appl. Phys.* **106** (2009) 114902.
- [5] Y. J. Lee *et al.*, *IEEE Electron Device Lett.* **34** (2013) 1286.
- [6] Chia-Pin Lin *et al.*, *IEEE EDL*. **27** (2006) 360.
- [7] Chen-Ming Lee *et al.*, *IEEE EDL*. **32** (2011) 327.
- [8] T. C. Lim *et al.*, *Solid-State Electron.* **50** (2006) 774.

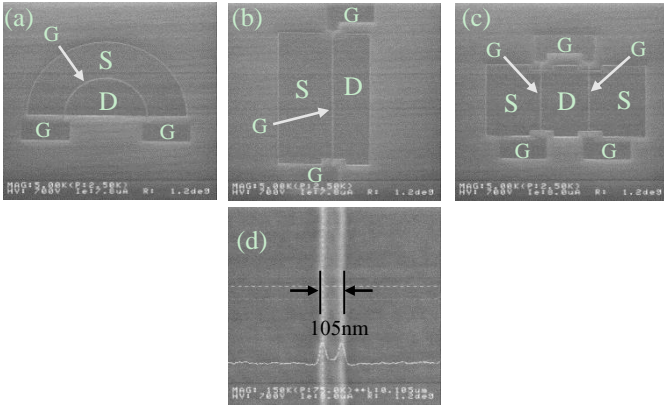


Fig. 1 Top-view SEM image of (a) annular, (b) single, (c) parallel, and (d) active region of poly-Si TFT with  $L = 105 \text{ nm}$ .

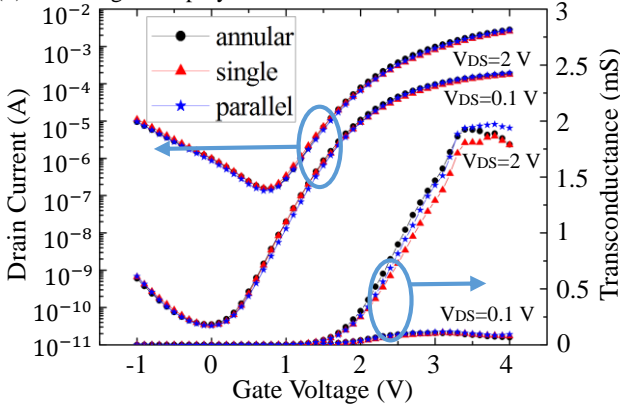


Fig. 2 The  $I_{DS} - V_{GS}$  transfer curves with different layout structures.

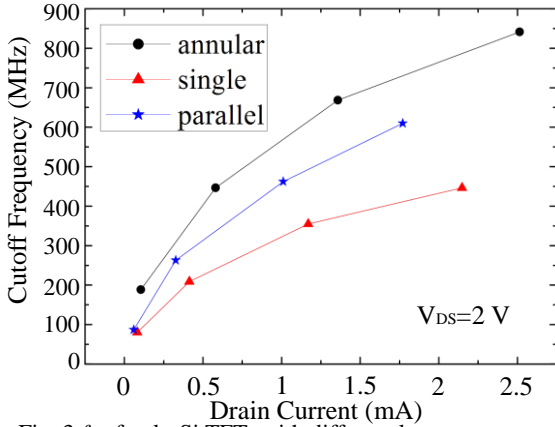


Fig. 3  $f_t$  of poly-Si TFTs with different layout structures.

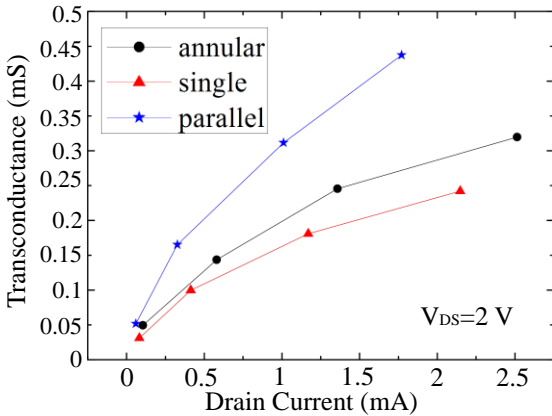


Fig. 4 Extracted transconductance of poly-Si TFTs with different layout structures.

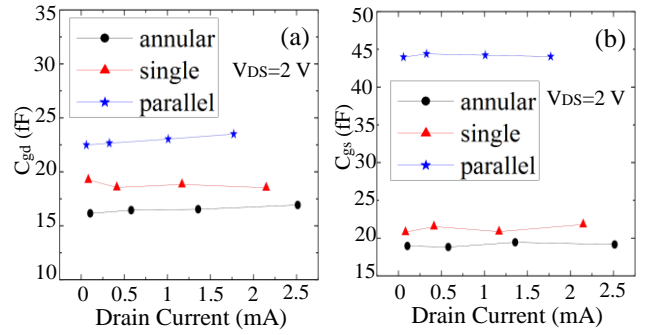


Fig. 5 Extracted (a)  $C_{gd}$  and (b)  $C_{gs}$  of poly-Si TFTs with different layout structures.

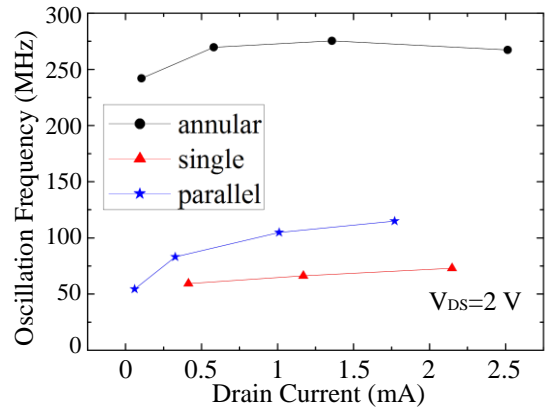


Fig. 6  $f_{max}$  of poly-Si TFTs with different layout structures.

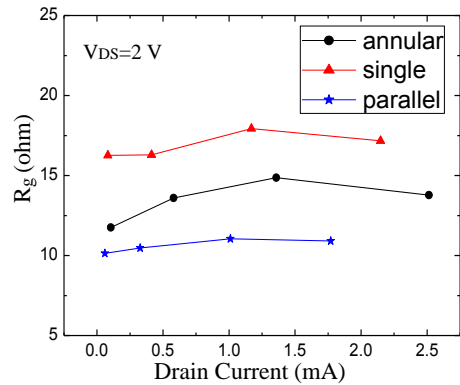


Fig. 7 Extracted  $R_g$  of poly-Si TFTs with different layout structures.

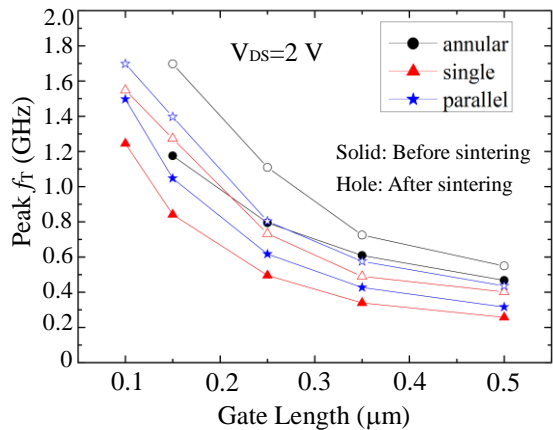


Fig. 8 Nonsintered and sintered peak  $f_t$  of poly-Si TFTs with different layout structures.